Interlobe Communication in Human Serum Transferrin: Metal Binding and Conformational Dynamics Investigated by Electrospray Ionization Mass Spectrometry†

Dmitry R. Gumerov,‡ Anne B. Mason,§ and Igor A. Kaltashov*,‡

Department of Chemistry, University of Massachusetts, 710 North Pleasant Street, Amherst, Massachusetts, 01003, and Department of Biochemistry, University of Vermont Medical School, 89 Beaumont Avenue, Burlington, Vermont 05405

Received November 18, 2002; Revised Manuscript Received March 7, 2003

ABSTRACT: Human serum transferrin (hTF) is an iron transport protein, comprising two lobes (N and C), each containing a single metal-binding center. Despite substantial structural similarity between the two lobes, studies have demonstrated the existence of significant differences in their metal-binding properties. The nature of these differences has been elucidated through the use of electrospray ionization mass spectrometry to study both metal retention and conformational properties of hTF under a variety of conditions. In the absence of chelating agents or nonsynergistic anions, the diferric form of hTF remains intact until the pH is lowered to 4.5. The monoferric form of hTF retains the compact conformation until the pH is lowered to 4.0, whereas the apoprotein becomes partially unfolded at pH as high as 5.5. Selective (lobe-specific) modulation of the iron-binding properties of hTF using recombinant forms of the protein (in which the pH-sensitive elements in each lobe were mutated) verifies that the N-lobe of the protein has a lower affinity for ferric ion. Surprisingly, the apo-N-lobe is significantly less flexible compared to the apo-C-lobe. Furthermore, the conformation of the iron-free N-lobe is stabilized when the C-lobe contains iron, confirming the existence of an interlobe interaction within the protein. The experimental results provide strong support for the earlier suggestion that hTF interacts with its receptor (TFR) primarily through the C-lobe both at the cell surface and inside the endosome.

Iron is one of the most abundant elements on earth and is critical to the life of all organisms. The unique electrochemical properties of the Fe^{2+}/Fe^{3+} couple have been widely utilized in a variety of metabolic processes (*1*). However, bioavailability of iron is limited, as the soluble ferrous ion (Fe^{2+}) becomes converted under aerobic conditions to Fe^{3+}, which forms an insoluble hydroxide at neutral pH. Therefore, the uptake, transport, and release of iron under physiological conditions each require specific carefully controlled mechanisms. Iron concentrations in body tissues must be tightly regulated because excessive iron leads to tissue damage through the formation of free radicals (*2*, *3*). Excess iron also stimulates the proliferation of a variety of pathogens, whose growth depends on the availability of this mineral (*4*). Sequestration and transport of iron in biological fluids of vertebrates are primarily carried out by transferrins, a family of monomeric glycoproteins (∼80 kDa) (*5*). Human serum transferrin (hTF)[1] has two structurally similar lobes, termed the N-lobe and the C-lobe, with each lobe containing one metal-binding center. An important feature of Fe^{3+} binding to each lobe of transferrin is the concurrent attachment of a synergistic anion (carbonate or oxalate), which provide two oxygen ligands needed to complete the octahedral coordination sphere (*6*). Recombinant transferrin N-lobe (hTF/2N) has been proven to be an excellent model for the N-lobe of intact transferrin (*6*). Delivery of ferric ion from plasma to tissue cells occurs via pH-dependent receptor-mediated endocytosis (*5*). Despite remarkable progress in the past decade toward understanding the mechanism of iron release from hTF during endocytosis, many details of this process remain uncertain. Mild acidification of the endosome is thought to play an important role in iron dissociation from hTF by activating the pH-sensitive triggers in each lobe, thereby forcing the protein to assume the "open" conformation (characteristic of the apo-form) (*7*). However, acidification to a typical endosomal level (pH 5.5) alone is not sufficient to cause dissociation of the metal−protein complex (*6*). We have recently demonstrated that acid-induced iron removal from the N-lobe of hTF (hTF/2N) in the absence of metal chelators and nonsynergistic anions

† This work was supported by National Institutes of Health Grants R01 GM61666 (I.A.K.) and R01 DK21739 (A.B.M.). D.R.G. acknowledges financial support from the Schering-Plough Corp. (Bioanalytical Fellowship).

* Author to whom correspondence should be addressed [telephone (413) 545-1460; fax (413) 545-4490; e-mail kaltashov@chem.umass.edu].

‡ University of Massachusetts.

§ University of Vermont.

[1] Abbreviations: TF, transferrin; TFR, transferrin receptor; hTF, human serum transferrin (wild type); hTF-NG, recombinant human serum transferrin (nonglycosylated); N-His-K206E-hTF-NG, recombinant human serum transferrin (nonglycosylated), in which the Lys-206 residue was substituted with Glu; N-His-K206E/K534A-hTF-NG, recombinant human serum transferrin (nonglycosylated), in which the Lys-206 residue was substituted with Glu and the Lys-534 residue with Ala; hTF/2N, N-lobe of human serum transferrin; ESI MS, electrospray ionization mass spectrometry; *m*/*z*, mass-to-charge ratio; citr, ammonium citrate.

10.1021/bi020660b CCC: $25.00
Published on Web 04/16/2003

occurs significantly below the endosomal pH and is accompanied by large-scale conformational changes (*8*). The observed conformational dynamics could not be described as a simple transition from the "closed" (holo) to the "open" (apo) form of the protein. The changes were attributed to a partial unfolding of the N-lobe. However, the presence of the iron chelator citrate at typical endogenous levels resulted in facile (although not complete) dissociation of the iron from the N-lobe at endosomal pH without protein unfolding (*8*).

Our long-term goal is to model the iron release from hTF by mimicking the in vivo conditions. Because the complex endosomal environment cannot be adequately modeled using a two-component solution (citrate and hTF/2N), we are beginning to introduce other components into the system. A specific goal of the present work is to study the metal-binding properties and conformational dynamics of each lobe of hTF in order to apply this knowledge to elucidation of the molecular mechanism of the hTF−TFR interaction. The two lobes of the protein are structurally similar [49% homology (*9*)] and are thought to have evolved from a single ancestral gene by duplication and fusion (*10*); however, some structural elements and the roles of the lobes in TFR recognition and binding appear to be rather different. These include a different number of disulfide bridges (8 in the N-lobe versus 11 in the C-lobe), and the two biantennary glycans which are N-linked to the C-lobe (*6*). Furthermore, a pH-dependent "dilysine trigger" (K206 and K296) plays a critical role in hTF/2N iron release, whereas a triad composed of K534, R632, and D634 serves as the pH-sensitive motif in the hTF/2C (*11*). Although the hTF−TFR binding depends on the two-domain structure of hTF (*12*), the iron-loaded C-lobe appears to serve as a major recognition site at extracellular pH (*13*, *14*). The cause of this asymmetry is not understood. Furthermore, it has been suggested that the endosomal pH forces TFR to change the binding preference (with the apo-hTF becoming the highest affinity ligand), thus shifting the equilibrium Fe_2hTF $\rightleftharpoons$ 2Fe + hTF toward iron release (*6*). Clearly, this affinity switch is difficult to understand or properly describe without considering the dynamic nature of iron binding and release.

Characterization of hTF dynamics is a challenging task, because the high molecular weight of the protein and the presence of high-spin Fe^{3+} cations render use of techniques such as high-resolution NMR impractical. X-ray crystallography is biased toward the most stable states of the protein and does not provide direct information on dynamic events. Electrospray ionization mass spectrometry (ESI MS) is increasingly being applied to study both the structure and the dynamics of non-covalent protein complexes (*15*−*17*). ESI is a gentle ionization method, yielding little or no fragmentation (unless specifically induced in the atmosphere/vaccuum interface) and has been used to detect intact weakly bound complexes. ESI MS has been particularly useful in the characterization of metalloproteins and metal−peptide complexes, including the determination of binding sites and stoichiometry, as well as ligand field geometry and composition (*18*−*23*). The potential of ESI MS to study protein conformational changes induced by metal ions has also been demonstrated (*8*, *24*−*26*). In the present work, we use ESI MS to monitor both the composition and conformational stability of hTF as a function of solution conditions. The results suggest the presence of significant interlobe communication within the protein, as well as anomalous flexibility of the apo-form of the protein C-lobe at endosomal pH, which may be critical for the interaction of hTF with its receptor as a function of pH.

EXPERIMENTAL PROCEDURES

Materials. Wild-type holo-hTF (polypeptide chain MW 79570) was purchased from Sigma Chemical Co. (St. Louis, MO). Recombinant nonglycosylated hTF (hTF-NG, MW 75143), as well as two mutants, N-His-K206E-hTF-NG and N-His-K206E/K534A-hTF-NG, were produced and purified as described in detail previously (*27*). All proteins were initially in the holo (diferric) form, as verified by ESI MS measurements. Apo-forms of the proteins were produced by dissolving 5 mg of lyophilized protein in 5 mL of H_2O/CH_3CO_2H/CH_3OH (47:3:50, v/v/v), followed by the addition of EDTA (to a final concentration of 1 mM). Each mixture was incubated at 36.4 °C for 3 h, followed by extensive ultrafiltration using a Centricon (10000 MWCO) microconcentrator (Millipore, Inc., Bedford, MA). Complete removal of metal ions from the protein samples was verified by ESI MS. All solvents, buffers, chelating agents, and other chemical reagents used in this work were of analytical grade or higher. To minimize the possibility of nonspecific metal−protein complex ion formation in the ESI interface, excess metal ions (low molecular weight complexes) were removed from solution prior to ESI MS measurements by extensive buffer exchange and ultrafiltration.

Mass Spectrometry. All mass spectra (positive ion mode) were acquired on a JMS-700 MStation (JEOL, Tokyo, Japan) two-sector mass spectrometer equipped with a standard ESI source. Protein samples were prepared for ESI MS analysis by diluting protein stock solutions (500 μM) in a 10 mM $CH_3CO_2NH_4$ buffer solution (the pH of which was adjusted to a desired level with NH_4OH or CH_3CO_2H) to a final protein concentration of 6 μM. All protein solutions were kept at room temperature (24 °C) prior to ESI analysis. To ensure equilibrium conditions in the protein solution during the ESI MS measurements, all pH adjustments for acid-induced iron release studies were carried out at least 3 h prior to MS experiments. The samples were introduced into the ESI source at flow rates of 3 μL/min. Full-range mass spectra were acquired by scanning the magnet at a 5 s/decade rate in the *m*/*z* range of 1000−5000 u. To ensure high signal-to-noise ratio and mass accuracy of the protein−metal ion stoichiometric measurements, second sets of spectra were acquired over a narrower range (typically 100 u) by averaging a greater number of scans.

In our previous studies of acid- and citrate-induced iron release from Fe•hTF/2N, moderate ESI source temperature (150 °C) and medium skimmer settings (half of the maximum potential) were determined to be optimal (as far as minimizing the alkali and acetate adduct formation while at the same time preserving the integrity of the [Fe^{3+}•$C_2O_4^{2-}$•hTF/2N] complex) (*8*). Higher skimmer potential leads to complete dissociation of a synergistic anion from the ternary complex (in the form of acid), whereas the ferric ion remains tightly bound to the protein ion even at the maximum skimmer potential. However, the mild "optimal" conditions were deemed to be impractical to study the dynamics of hTF due to the high mass of the protein (~80 kDa). Calculated protein

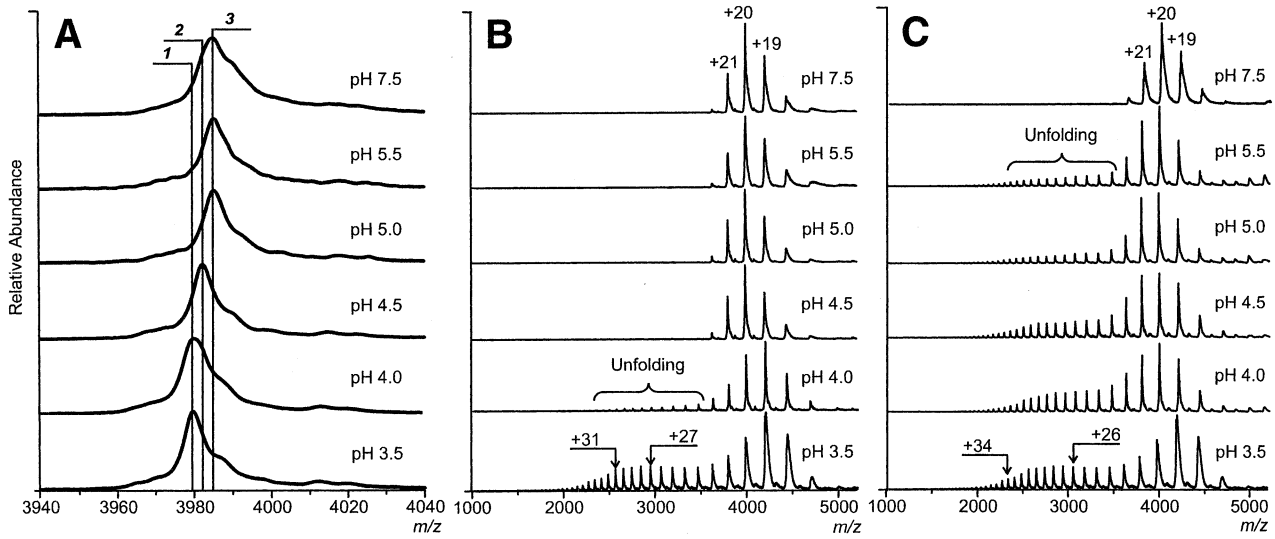

FIGURE 1: ESI mass spectra of holo-hTF (A, B) and apo-hTF (C) acquired in the pH range of 3.5−7.5. Panel A contains narrow-range mass spectra showing zoomed peak shapes (ionic species labeled as follows: 1, $[M + 20H^+]^{20+}$; 2, $[M + Fe^{3+} + 17H^+]^{20+}$; and 3, $[M + 2Fe^{3+} + 14H^+]^{20+}$).

Table 1: Conformational and Compositional Changes of HTF/2N, wt-hTF, N-His-K206E-hTF-NG, and N-His-K206E/K534A-hTF-NG as a Function of pH

	hTF/2N		wt-hTF		N-His-K206E-hTF-NG	N-His-K206E/K534A-hTF-NG
pH	apo	holo	apo	holo	holo	holo
7.0	$[hTF/2N]^{fold}$	$[Fe^{3+}\cdot hTF/2N]^{fold}$	$[hTF]^{fold}$	$[Fe_2^{3+}\cdot hTF]^{fold}$	$[Fe_2^{3+}\cdot hTF]^{fold}$	$[Fe_2^{3+}\cdot hTF]^{fold}$
5.5	$[hTF/2N]^{fold}$	$[Fe^{3+}\cdot hTF/2N]^{fold}$	$[hTF]^{fold}$ $[hTF]^{unfold}$	$[Fe_2^{3+}\cdot hTF]^{fold}$	$[Fe_2^{3+}\cdot hTF]^{fold}$	$[Fe_2^{3+}\cdot hTF]^{fold}$
4.5	$[hTF/2N]^{fold}$ $[hTF/2N]^{unfold}$	$[Fe^{3+}\cdot hTF/2N]^{fold}$ $[hTF/2N]^{fold}$ $[hTF/2N]^{unfold}$	$[hTF]^{fold}$ $[hTF]^{unfold}$	$[Fe_2^{3+}\cdot hTF]^{fold}$ $[Fe_1^{3+}\cdot hTF]^{fold}$	$[Fe_2^{3+}\cdot hTF]^{fold}$	$[Fe_2^{3+}\cdot hTF]^{fold}$
4.0	$[hTF/2N]^{fold}$ $[hTF/2N]^{unfold}$	$[hTF/2N]^{fold}$ $[hTF/2N]^{unfold}$	$[hTF]^{fold}$ $[hTF]^{unfold}$	$[Fe_1^{3+}\cdot hTF]^{fold}$ $[hTF]^{fold}$ $[hTF]^{unfold}$	$[Fe_1^{3+}\cdot hTF]^{fold}$ $[hTF]^{fold}$ $[hTF]^{unfold}$	$[Fe_2^{3+}\cdot hTF]^{fold}$
3.5	$[hTF/2N]^{fold}$ $[hTF/2N]^{unfold}$	$[hTF/2N]^{fold}$ $[hTF/2N]^{unfold}$	$[hTF]^{fold}$ $[hTF]^{unfold}$	$[hTF/2N]^{fold}$ $[hTF/2N]^{unfold}$	$[hTF/2N]^{fold}$ $[hTF/2N]^{unfold}$	$[hTF/2N]^{fold}$ $[hTF/2N]^{unfold}$

ion peak widths (based on the natural isotopic abundance) far exceeded the mass difference between Fe and carbonate (the synergistic anions), thus making it impossible to differentiate among various possible intermediate forms of the complex [e.g., $[(Fe^{3+})_N\cdot(Fe^{3+})_C\cdot hTF]$ and putative $[(Fe^{3+}\cdot CO_3^{2-})_C\cdot hTF]$ (Supporting Information, Figure 1)]. Therefore, in the present work we have chosen to study hTF dynamics under maximum skimmer conditions to ensure removal of the synergistic anion from the protein−metal ion complex in the gas phase. This simplifies the interpretation of ESI spectra of hTF, because only three ionic species can be detected under these conditions: $[(Fe^{3+})_2\cdot hTF]$, $[Fe^{3+}\cdot hTF]$, and hTF.

Calculation of Protein Solvent-Accessible Surface Area. Protein solvent-exposed surface areas were approximated using GETAREA 1.1 software (available from http://www.scsb.utmb.edu/getarea/area_form.html). A 1.4 Å probe radius was used for calculations.

RESULTS

Acid-Induced Iron Release from hTF. Ferric ions bind to hTF very tightly at physiological pH (effective formation constants for blood plasma $K_1 = 7 \times 10^{22}$ and $K_2 = 4 \times 10^{21}$) (*7*). Mild acidification of the endosome to pH 5.5 (following activation of ATP-driven proton pumps) is a major factor facilitating iron release from hTF during receptor-mediated endocytosis. The ESI spectrum of holo-hTF acquired at physiological pH indicates that the protein exists exclusively in the form of a diferric complex, $[Fe_2\cdot hTF]$ (Figure 1A). Consistent with the results of earlier spectroscopic studies, no noticeable release of ferric ion from the protein is observed when the solution pH is lowered to a typical endosomal level of 5.5 (*5*, *7*). Importantly, the protein retains a compact tightly folded conformation at this pH, as suggested by the appearance of the protein ion charge state distributions in the ESI spectra (a single narrow distribution at high *m*/*z*). The onset of iron release from the protein does not occur until the pH is lowered to 4.5, at which point a monoferric form of the protein is observed in the ESI spectrum. Dissociation of the second ferric ion (to yield the apo-form of the protein) takes place at pH 4.0 (Figure 1A).

An intriguing feature of the ESI spectrum acquired at pH 4.0 is the presence of a high charge state (low *m*/*z*) distribution of protein ion peaks, which become more pronounced as the solution pH is lowered further (Figure 1B). These ion peaks corespond to the apo-form of the protein (Table 1). Emergence of such high-charge density protein ion distributions usually indicates a large-scale conformational change occurring within the protein, as less structured protein conformations can accommodate a greater number

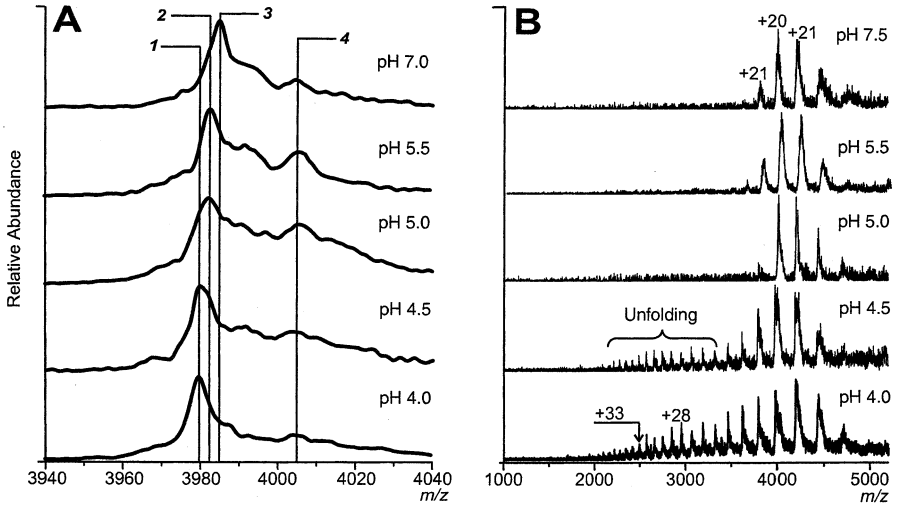

FIGURE 2: ESI mass spectra of holo-hTF acquired in the pH range of 4.0−7.0 in the presence of 0.15 mM ammonium citrate, $(NH_4)_2C_6H_6O_7$. Panel A contains narrow-range mass spectra showing zoomed peak shapes (ionic species labeled as follows: 1, $[M + 20H^+]^{20+}$; 2, $[M + Fe^{3+} + 17H^+]^{20+}$; 3, $[M + 2Fe^{3+} + 14H^+]^{20+}$; and 4, $[M + 2Fe^{3+} + C_6H_6O_7^{2} + 16H^+]^{20+}$).

of charges during the ESI process compared to the tightly folded (compact) states of the same protein (*28*, *29*). Therefore, the observed behavior of hTF ions most likely reflects partial unfolding of the protein at mildly acidic pH. An alternative interpretation invoking the conformational switch from the "closed" (holo) to the "open" (apo) form of the protein upon iron release does not seem feasible. Although these two conformations differ significantly (*30*), both are tightly folded and transition from one to another does not result in a significant change of the solvent-exposed surface area of the protein [a major determinant of the extent of multiple charging of protein ions (*29*, *31*, *32*)]. Indeed, a transition from the holo- to the apo-form of duck ovotransferrin results in a small (~5%) increase of the solvent-accessible area, which is expected to cause an average charge state shift in the ESI MS spectra of no greater than 2% (*33*). Duck ovotransferrin was used in these calculations because this protein is highly homologous to hTF and crystal structures for both apo- and holo-forms of duck ovotransferrin are currently available (*34*, *35*) (no crystal structures of intact hTF are available at present). Furthermore, the protein ion charge-state distributions in the ESI spectra of holo- and apo-forms of hTF acquired under near-native conditions (pH 7.5) were nearly identical (Figure 1B,C), suggesting that the small difference in solvent-exposed areas of the two forms of the protein is beyond detection limits of ESI MS.

The ESI spectra of apo-hTF acquired within a wide range of pH indicate that the large-scale conformational changes occur at a pH as high as 5.5 (Figure 1C). This is in sharp contrast with the behavior of the diferric form of hTF (unfolding does not occur until the pH is lowered to 4.0, vide infra). Importantly, our earlier studies of acid unfolding of apo-hTF/2N suggested that the protein undergoes large-scale conformational changes at pH 4.5 [which is also a threshold pH for the release of iron from the holo-form of hTF/2N (*8*)].

Iron Removal from Fe_2hTF in the Presence of Citrate. Metal chelators and nonsynergistic anions are known to facilitate Fe^{3+} dissociation from holo-TF (*6*). Citrate does not compromise the integrity of the Fe_2hTF at extracellular pH, as evidenced by the appearance of the ESI spectrum acquired at pH 7.5 (Figure 2). At the same time, the ESI spectrum of holo-hTF acquired at pH 5.5 in the presence of 0.15 mM citrate indicates that removal of one ferric ion becomes very efficient once the pH is lowered to the endosomal level. Dissociation of the second ferric ion does not commence until the pH is lowered to 4.5. Large-scale conformational changes become evident at this pH, as suggested by the emergence of protein ion peaks at low *m*/*z* (Figure 2B). Although the dissociation of the second ferric ion from hTF in the absence of citrate occurred at lower pH (vide infra), it was also accompanied by (partial) protein unfolding. Therefore, it appears that the two events (complete dissociation of iron from the protein and protein unfolding) are correlated, suggesting that the most tightly bound ferric ion is an essential determinant of the protein stability.

Selective Modulation of Iron-Binding Capacity and Its Effect on Protein Stability. Despite a very high degree of sequence homology, a suspected common origin, and significant structural similarity of the metal-binding centers of the two lobes of hTF, their iron-binding properties are quite different (*6*). The C-lobe of the protein is known to have a higher affinity for Fe^{3+}. Therefore, the stepwise dissociation of Fe_2hTF, observed in this work, most likely reflects asymmetry in iron retention by the two lobes of the protein (with initial dissociation of Fe^{3+} from the N-lobe of the protein at pH 4.5, followed by iron release from the C-lobe at pH 4.0). The ferric ion affinity of each lobe can be selectively modulated in a pH-sensitive fashion by mutations that affect (i) the ligand field composition (amino acid residues coordinating Fe^{3+}) or (ii) the residues triggering the switch between the closed (holo) and open (apo) forms of each lobe of the protein. The former mutations usually reduce the metal-binding capability, whereas the latter ones may increase Fe^{3+} affinity very significantly. The protein is particularly sensitive to mutations of one or more amino acid residues forming the so-called dilysine trigger (*7*). Thus, abolition of the dilysine trigger in the hTF/2N (by mutating one or both of the participating lysine residues, Lys-206 or Lys-296, to a nonbasic residue) results in a much greater stability of the Fe·hTF/2N complex at mildly acidic condi-

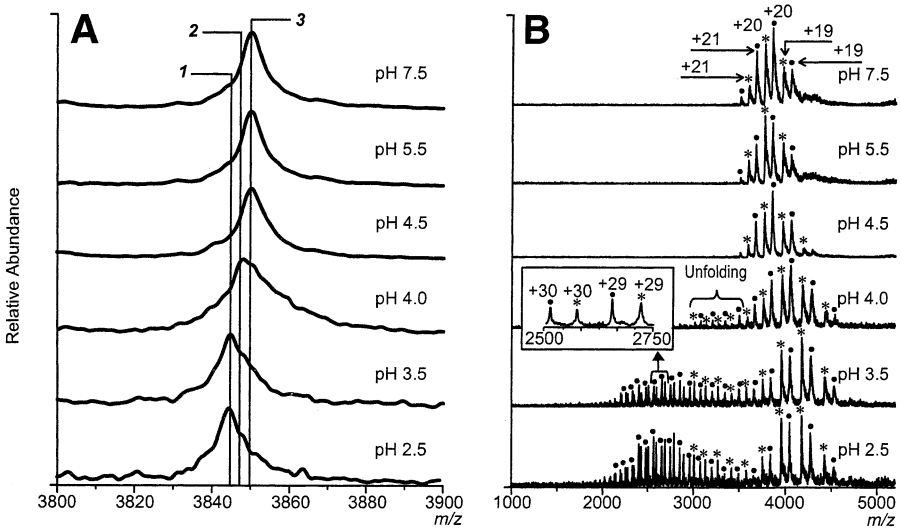

FIGURE 3: ESI mass spectra of holo-N-His-K206E-hTF-NG acquired in the pH range of 2.5−7.5. The protein sample is a nearly equimolar mixture of two isoforms (with and without an N-terminal His-tag, VPDLHHHHHHIGER). Ion peaks corresponding to different protein isoforms are labeled with * (no His-tag) and ● (His-tag attached). Panel A contains narrow-range mass spectra showing zoomed peak shapes of the His-tag-free isoform (ionic species labeled as follows: 1, $[M + 20H^+]^{20+}$; 2, $[M + Fe^{3+} + 17H^+]^{20+}$; and 3, $[M + 2Fe^{3+} + 14H^+]^{20+}$).

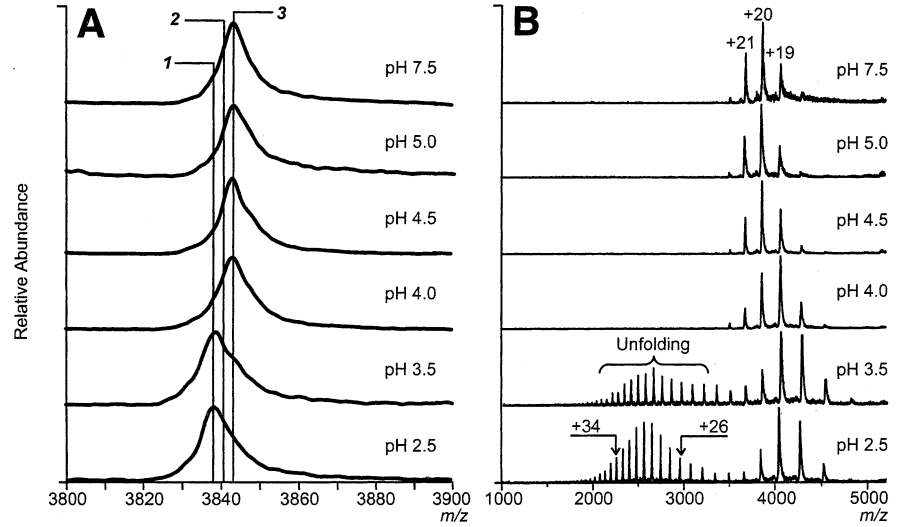

FIGURE 4: ESI mass spectra of holo-N-His-K206E/K534A-hTF-NG acquired in the pH range of 2.5−7.5. Panel A contains narrow-range mass spectra showing zoomed peak shapes (ionic species labeled as follows: 1, $[M + 20H^+]^{20+}$; 2, $[M + Fe^{3+} + 17H^+]^{20+}$; and 3, $[M + 2Fe^{3+} + 14H^+]^{20+}$).

tions (*36*). Likewise, abolition of the triad in the C-lobe (Lys-534, Arg-632, or Asp-634) greatly enhances its iron-binding capacity in the pH range 4.5−6.5 (*27*).

To explore the correlation between the protein conformational stability and ferric ion binding (in a lobe-specific fashion), two hTF mutants were used: N-His-K206E-hTF-NG and N-His-K206E/K534A-hTF-NG. The first mutant leads to enhanced binding of iron to the N-lobe alone, whereas the latter increases the strength of binding in both lobes. ESI MS spectra of the holo form of N-His-K206E-hTF-NG show no sign of iron release in the pH range from 7.5 to 4.5 (Figure 3). The protein releases a single ferric ion only when the pH is lowered to 4.0. The transition from the diferric to monoferric form of the protein is accompanied by (partial) unfolding of the protein (Figure 4B). The apo-form of N-His-K206E-hTF-NG is not observed until the pH is lowered to 3.5 (Figure 4A). ESI spectra of the holo-form of the double mutant, N-His-K206E/K534A-hTF-NG (increased Fe^{3+}-binding capacity of both lobes of the protein), indicate that both ferric ions are retained by the protein in the pH range from 7.5 to 4.0 (Figure 4). Transformation of the diferric form of the protein to its apo-form occurs within a narrow pH range (from 4.0 to 3.5) and is accompanied by protein unfolding. These results are summarized in Table 1.

Potential Role of Glycans and an N-Teminal His-tag in Modulating Protein Iron-Binding Properties and Conformational Stability. The experiments presented in the previous section clearly establish a correlation between ferric ion retention in the C-lobe of the protein and its conformational stability. However, it must be pointed out that the mutations of Lys-206 and Lys-534 are not the only structural differences between the wild-type protein (hTF) and the mutant proteins. The wild-type protein is glycosylated (two N-linked biantennary glycans are located in the C-lobe of the protein at positions Asn-413 and Asn-611), whereas both mutants contain Asp residues at these positions and are

thus nonglycosylated. The capacity of Asn-linked glycans to influence protein structure and folding is well-documented (*37*−*39*). Therefore, it is possible that some of the differences in the conformational and iron-binding properties between hTF and the mutants may be attributed to the absence of the carbohydrate or to the presence of a His-tag at the amino terminus. To test for the effect of the glycan presence, an ESI MS study of acid-induced iron release and conformational dynamics of the nonglycosylated form of hTF (hTF-NG) was carried out (Supporting Information, Figure 2). No differences in iron-binding properties were detected between hTF and hTF-NG. Likewise, the conformational dynamics of the two forms of hTF appear to be identical under the conditions used in our studies (Figure 1; Supporting Information, Figure 2). The mutant constructs used in this work also differ from both the wild-type protein and hTf-NG by the presence of the His-tags on the N termini. It has been shown recently that His-tags may exert certain influence on the kinetics of transferrin−metal interactions (*40*). To ensure that the presence of the His-tags did not affect the equilibrium measurements of Fe^{3+} release from the protein in the present work, acid-induced metal release studies were carried out with a mixture of two proteins, N-His-K206E-hTF-NG and K206E-hTF-NG. This mixture was prepared by partial removal of the His-tag from the N-His-K206E-hTF-NG construct. The identical behaviors of these proteins vis a vis metal ion dissociation and partial structure loss (Figure 3) clearly indicate that the N-terminal His-tag has no effect on the conformational or iron-binding properties of the mutant.

These experiments provide conclusive evidence that the observed changes in iron-binding properties and conformational stability of the two mutants (as compared to hTF) are fully attributable to the abolition of the pH-sensitive motifs, and not to the change in the glycosylation or the presence of the His-tag at the amino terminus.

DISCUSSION

The ESI MS study of acid-induced iron release from the holo-form of hTF suggests that dissociation of ferric ion from the protein occurs in a stepwise fashion, and the transition from the monoferric to the apo-form is accompanied by a (partial) unfolding of the protein (the notation of the synergistic anion is omitted here):

$$[Fe_2^{3+}\cdot hTf] \xrightarrow{pH\ 4.5} [Fe^{3+}\cdot hTf] \xrightarrow{pH\ 4.0} [hTf] \rightleftharpoons [hTf]^{unfold} \quad (1)$$

Previous spectrophotometric studies established that the C-lobe of hTF has higher ferric ion affinity (as compared to the N-lobe) and releases iron at a lower pH (*41*). Our own earlier studies of acid-induced iron release from hTF/2N also suggested that the dissociation of ferric ion from the N-lobe of hTF occurs at pH 4.5 (*8*):

$$[Fe^{3+}\cdot hTf/2N] \xrightarrow{pH\ 4.5} [hTf/2N] \rightleftharpoons [hTf/2N]^{unfold} \quad (2)$$

This allows us to assign the initial step in eq 1 as Fe^{3+} dissociation from the N-lobe of hTF, that is eq 1 can be modified as

$$[Fe_2^{3+}\cdot hTf] \xrightarrow{pH\ 4.5} [(Fe^{3+})_c\cdot hTf] \xrightarrow{pH\ 4.0} [hTf] \rightleftharpoons [hTf]^{unfold} \quad (3)$$

Importantly, acid-induced dissociation of ferric ion from the N-lobe of hTF (unlike iron removal from hTF/2N) does not result in large-scale conformational changes, whereas Fe^{3+} dissociation from the C-lobe of the protein is accompanied by partial protein unfolding. This surprising conclusion is corroborated by the results of the small-angle X-ray solution scattering studies of hTF, which indicated that the protein radius of gyration (R_g) remains effectively constant in the pH range associated with iron release from the N-lobe, whereas the complete release of iron from the protein resulted in a very significant increase in its R_g (*42*). Interestingly, model simulations suggested that the opening of the metal-binding cleft in the C-lobe of the protein (via rotation of the CII domain parallel with the Fe^{3+}-binding site plane) can only partially account for the measured increase in R_g. No reasonable combined repositioning of the NII and CII domains was consistent with the experimentally observed increase in R_g. This apparent anomaly can now be attributed to the partial protein unfolding. Indeed, the large-scale conformational change, which accompanies iron release from the C-lobe of the protein, would most certainly result in a significant increase of the R_g. The measured R_g in a multicomponent system is determined as

$$R_g^{meas} = \sqrt{\sum_i f_i (R_g^i)^2} \quad (4)$$

(where f_i is a fractional concentration of a conformer i), hence the increase of the measured radius of gyration due to the contribution from the (partially) unstructured state(s) of the apo-hTF.

Studies of citrate-induced iron release from hTF provide further evidence that the (partial) protein unfolding is linked to the dissociation of Fe^{3+} from the C-lobe of the protein. In this case, facilitation of iron release results in decreased conformational stability:

$$[Fe_2^{3+}\cdot hTf] \xrightarrow{pH\ 5.5,\ citr} [(Fe^{3+})_c\cdot hTf] \xrightarrow{pH\ 4.5,\ citr} [hTf] \rightleftharpoons [hTf]^{unfold} \quad (5)$$

Furthermore, the apo-form of hTF is significantly less stable, as compared to the apo-form of the N-lobe hTF/2N, with the difference in the onset of acid-induced unfolding shifted by 1 pH unit:

$$[hTf] \overset{pH\ 5.5}{\rightleftharpoons} [hTf]^{unfold} \quad (6)$$

$$[hTf/2N] \overset{pH\ 4.5}{\rightleftharpoons} [hTf/2N]^{unfold} \quad (7)$$

If the iron release pathways from hTF are adequately described by eqs 3 and 5, then any enhancement of Fe^{3+} binding by the N-lobe should not have any effect on the onset of the acid-induced unfolding of the protein. In contrast to this, modulation of Fe^{3+} affinity of the C-lobe of the protein at pH 5.5 and below should shift the onset of protein unfolding. The experimental data collected for the N-His-K206E-hTF-NG and N-His-K206E/K534A-hTF-NG mutants suggest that this is the case. Abolition of the dilysine trigger in the N-lobe leads to a very significant enhancement of iron retention by the protein, but it does not affect the onset of the protein unfolding (Figure 3). On the other hand, abolition

of the pH-sensitive motifs in each lobe results in both increased iron-binding capacity and enhanced conformational stability of the protein at mildly acidic pH (Figure 4).

Dual Role of the C-lobe: Intrinsic Disorder of the Apo-form and Stabilization of the N-lobe by the Holo-form. The picture of the behavior of hTF that emerges from analysis of acid-induced iron release studies and from the conformational dynamics work is very interesting. The two lobes of the protein appear to be rather autonomous, although they do interact with each other in a very interesting fashion. The dual role of the C-lobe appears to be particularly intriguing. Thus, the metal-loaded C-lobe reduces the conformational flexibility of the metal-free N-lobe (compare eqs 2 and 3). At the same time, the apo-form of the C-lobe is significantly more flexible (i.e., it unfolds at higher pH) than the iron-free N-lobe. Such behavior of the C-lobe may have very important implications for the TF−TFR interaction at both extracellular and endosomal conditions. The C-lobe serves as a primary recognition site for TFR (*13*). Therefore, the anomalous flexibility of the C-lobe may have important implications for the TF−TFR interaction at both extracellular and endosomal conditions. This is true particularly when one considers that increased intrinsic plasticity is often a prerequisite for effective molecular recognition (*43*−*47*). A recent report by Zak et al. (*14*) suggests that the apo-form of the C-lobe has increased flexibility. Therefore, it appears that the structural plasticity of the C-lobe may be an important determinant of the receptor-assisted iron release. Indeed, the apo-form of hTF is not recognized by the TFR at the extracellular pH of 7.4; however, it binds tightly to the receptor at the endosomal pH of 5.5 (*6*). This suggests that TFR may act as a facilitator of iron release from hTF inside the endosome, serving as a macromolecular transducer in an "induced fit" type of interaction (i.e., by changing its own conformation and thus forcing a transition of hTF from the closed to the open conformation). Flexibility of the iron-free C-lobe demonstrated in the present work would then be crucial for adaptation of hTF to the putative "acidic" conformation of TFR, thus making the entire transformation "conformational switch−affinity switch" a very efficient process.

The N-lobe of hTF is thought to play a secondary role in hTF−TFR interactions, enhancing the hTF binding to the receptor following the initial recognition event (*12*, *13*). Therefore, the stabilizing influence of the iron-loaded C-lobe on the conformation of the N-lobe may be critical for maintaining the integrity of the [$(Fe^{3+})_C$·hTF-TFR] complex during the initial stages of endocytosis. Interlobe interaction in hTF has been suggested previously on the basis of the results of ^1H, ^{13}C NMR studies of Ga^{3+} uptake by hTF (*48*), mutagenesis of the Asp ligands in both Fe^{3+}-binding sites of hTF (*49*), calorimetry studies, and recent work in which the addition of a hexahistidine tag to the carboxy terminus of hTF affected iron release from both the N- and C-lobes.

CONCLUSIONS

Our experimental results provide insight into the asymmetric roles played by the two lobes of hTF in metal binding and receptor recognition. Although both diferric (i.e., [$(Fe^{3+})_N$·$(Fe^{3+})_C$·hTF]) and monoferric (i.e., [$(Fe^{3+})_C$·hTF]) forms of the protein retain compact conformations, a fraction of the apo-form of the protein is unfolded at pH 5.5 and below. Although the iron-free C-lobe exhibits an anomalous conformational plasticity, the conformation of the apo N-lobe is actually stabilized when a ferric ion is present in the C-lobe. The specific structural details dictating the mechanisms of such asymmetric interlobe interaction have yet to be elucidated. The results provide support for the earlier suggestions that hTF interacts with its receptor (TFR) primarily through the C-lobe (*13*, *14*). The observed flexibility of the apo-form of the C-lobe at the endosomal pH may be an important factor facilitating efficient adaptation of the apo-form of the protein to a putative "acidic" conformation of TFR inside the endosome. This, in turn, may be an important factor directing efficient in vivo iron release from hTF in the endosome.

ACKNOWLEDGMENT

We thank Dr. Stephen J. Eyles (University of Massachusetts) for his valuable input.

SUPPORTING INFORMATION AVAILABLE

Figures showing ESI mass spectra of holo-hTF, holo-hTF-NG, and apo-hTF-NG. This material is available free of charge via the Internet at http://pubs.acs.org.

REFERENCES

1. Crichton, R. (2001) *Inorganic Biochemistry of Iron Metabolism: from Molecular Mechanisms to Clinical Consequences*, 2nd ed., Wiley, Chichester, U.K.
2. McCord, J. M. (1998) *Semin. Hematol. 35*, 5−12.
3. Emerit, J., Beaumont, C., and Trivin, F. (2001) *Biomed. Pharmacother. 55*, 333−339.
4. Jurado, R. L. (1997) *Clin. Infect. Dis. 25*, 888−895.
5. Aisen, P. (1998) *Met. Ions Biol. Syst. 35*, 585−631.
6. Sun, H. L. H., and Sadler, P. J. (1999) *Chem. Rev. 99*, 2817−2842.
7. He, Q. Y., Mason, A. B., Tam, B. M., MacGillivray, R. T., and Woodworth, R. C. (1999) *Biochemistry 38*, 9704−9711.
8. Gumerov, D. R., and Kaltashov, I. A. (2001) *Anal. Chem. 73*, 2565−2570.
9. Baldwin, G. S. (1993) *Comp. Biochem. Physiol. B 106*, 203−218.
10. Bruns, C. M., Nowalk, A. J., Arvai, A. S., McTigue, M. A., Vaughan, K. G., Mietzner, T. A., and McRee, D. E. (1997) *Nat. Struct. Biol. 4*, 919−924.
11. Dewan, J. C., Mikami, B., Hirose, M., and Sacchettini, J. C. (1993) *Biochemistry 32*, 11963−11968.
12. Mason, A. B., Tam, B. M., Woodworth, R. C., Oliver, R. W., Green, B. N., Lin, L. N., Brandts, J. F., Savage, K. J., Lineback, J. A., and MacGillivray, R. T. (1997) *Biochem. J. 326*, 77−85.
13. Zak, O., Trinder, D., and Aisen, P. (1994) *J. Biol. Chem. 269*, 7110−7114.
14. Zak, O., Ikuta, K., and Aisen, P. (2002) *Biochemistry 41*, 7416−7423.
15. Loo, J. A. (1997) *Mass Spectrom. Rev. 16*, 1−23.
16. Hernandez, H., and Robinson, C. V. (2001) *J. Biol. Chem. 276*, 46685−46688.
17. Kaltashov, I. A., and Eyles, S. J. (2002) *Mass Spectrom. Rev. 21*, 37−71.
18. Kaltashov, I. A., Cotter, R. J., Feinstone, W. H., Ketner, G. W., and Woods, A. S. (1997) *J. Am. Soc. Mass Spectrom. 8*, 1070−1077.
19. Fabris, D., and Fenselau, C. (1999) *Anal. Chem. 71*, 384−387.
20. Kuchumov, A. R., Loo, J. A., and Vinogradov, S. N. (2000) *J. Protein Chem. 19*, 139−149.
21. Ngoka, L. C., and Gross, M. L. (2000) *J. Mass Spectrom. 35*, 265−276.
22. Johnson, K. A., Verhagen, M. F., Brereton, P. S., Adams, M. W., and Amster, I. J. (2000) *Anal. Chem. 72*, 1410−1418.
23. Afonso, C., Hathout, Y., and Fenselau, C. (2002) *J. Mass Spectrom. 37*, 755−759.

24. Nemirovskiy, O., Giblin, D. E., and Gross, M. L. (1999) *J. Am. Soc. Mass Spectrom. 10*, 711−718.
25. Wang, F., Li, W., Emmett, M. R., Marshall, A. G., Corson, D., and Sykes, B. D. (1999) *J. Am. Soc. Mass Spectrom. 10*, 703−710.
26. van den Bremer, E. T., Jiskoot, W., James, R., Moore, G. R., Kleanthous, C., Heck, A. J., and Maier, C. S. (2002) *Protein Sci. 11*, 1738−1752.
27. Halbrooks, P. J., He, Q.-Y., Briggs, S. K., Everse, S. J., Smith, V. C., MacGillivray, R. T. A., and Mason, A. B. (2003) *Biochemistry 42*, 3701−3707.
28. Konermann, L., Rosell, F. I., Mauk, A. G., and Douglas, D. J. (1997) *Biochemistry 36*, 6448−6456.
29. Dobo, A., and Kaltashov, I. A. (2001) *Anal. Chem. 73*, 4763−4773.
30. Jeffrey, P. D., Bewley, M. C., MacGillivray, R. T., Mason, A. B., Woodworth, R. C., and Baker, E. N. (1998) *Biochemistry 37*, 13978−13986.
31. Fenn, J. B. (1993) *J. Am. Soc. Mass Spectrom. 4*, 524−535.
32. Konermann, L., and Douglas, D. J. (1997) *Biochemistry 36*, 12296−12302.
33. Mohimen, A., Dobo, A., and Kaltashov, I. A. Manuscript in preparation.
34. Rawas, A., Moreton, K., Muirhead, H., and Williams, J. (1989) *J. Mol. Biol. 208*, 213−214.
35. Rawas, A., Muirhead, H., and Williams, J. (1996) *Acta Crystallogr. D Biol. Crystallogr. 52*, 631.
36. Nurizzo, D., Baker, H. M., He, Q. Y., MacGillivray, R. T., Mason, A. B., Woodworth, R. C., and Baker, E. N. (2001) *Biochemistry 40*, 1616−1623.
37. Rudd, P. M., and Dwek, R. A. (1997) *Crit. Rev. Biochem. Mol. Biol. 32*, 1−100.
38. Imperiali, B., and O'Connor, S. E. (1999) *Curr. Opin. Chem. Biol. 3*, 643−649.
39. O'Connor, S. E., Pohlmann, J., Imperiali, B., Saskiawan, I., and Yamamoto, K. (2001) *J. Am. Chem. Soc. 123*, 6187−6188.
40. Mason, A. B., He, Q. Y., Halbrooks, P. J., Everse, S. J., Gumerov, D. R., Kaltashov, I. A., Smith, V. C., Hewitt, J., and MacGillivray, R. T. (2002) *Biochemistry 41*, 9448−9454.
41. Aisen, P., Leibman, A., and Zweier, J. (1978) *J. Biol. Chem. 253*, 1930−1937.
42. Mecklenburg, S. L., Donohoe, R. J., and Olah, G. A. (1997) *J. Mol. Biol. 270*, 739−750.
43. Luque, I., and Freire, E. (2000) *Proteins S4*, 63−71.
44. Tsai, C. J., Ma, B., Sham, Y. Y., Kumar, S., and Nussinov, R. (2001) *Proteins 44*, 418−427.
45. Tsai, C. D., Ma, B., Kumar, S., Wolfson, H., and Nussinov, R. (2001) *Crit. Rev. Biochem. Mol. Biol. 36*, 399−433.
46. Demchenko, A. P. (2001) *J. Mol. Recognit. 14*, 42−61.
47. Luque, I., Leavitt, S. A., and Freire, E. (2002) *Annu. Rev. Biophys. Biomol. Struct. 31*, 235−256.
48. Beatty, E. J., Cox, M. C., Frenkiel, T. A., Tam, B. M., Mason, A. B., MacGillivray, R. T., Sadler, P. J., and Woodworth, R. C. (1996) *Biochemistry 35*, 7635−7642.
49. Mason, A., He, Q. Y., Tam, B., MacGillivray, R. A., and Woodworth, R. (1998) *Biochem. J. 330*, 35−40.

BI020660B